

Physicochemical and Functional Comparability Between the Proposed Biosimilar Rituximab GP2013 and Originator Rituximab

Jan Visser · Isabel Feuerstein · Thomas Stangler ·
Timo Schmiederer · Cornelius Fritsch ·
Martin Schiestl

Published online: 7 May 2013

© The Author(s) 2013. This article is published with open access at Springerlink.com

Abstract

Background Regulatory approval for a biosimilar product is provided on the basis of its comparability to an originator product. A thorough physicochemical and functional comparability exercise is a key element in demonstrating biosimilarity. Here we report the characterization of a proposed biosimilar rituximab (GP2013) and originator rituximab.

Objective To compare GP2013 with originator rituximab using an extensive array of routine analytical and extended characterization methods.

Methods Primary and higher order protein structures were analyzed using a variety of methods that included high-performance liquid chromatography electrospray ionization mass spectrometry (HPLC-ESI-MS), peptide mapping with UV and MS detection, circular dichroism (CD), Fourier transform infrared (FTIR) spectroscopy, hydrogen deuterium exchange (HDX) MS, 1D ^1H nuclear magnetic resonance (NMR) spectroscopy, X-ray crystallography and differential scanning calorimetry (DSC). Charge and amino acid modifications were assessed using cation exchange chromatography (CEX) and peptide mapping using reversed-phase (RP) HPLC. Boronate affinity chromatography was used to determine the relative amount of glycation. Glycans were identified and quantified after 2-aminobenzamide (2-AB) labeling and

separation using normal phase HPLC with fluorescence and MS detection, respectively. Glycan site occupancy was determined using reducing capillary electrophoresis with sodium dodecyl sulfate (CE-SDS). Size heterogeneity was determined using reducing and non-reducing CE-SDS, size exclusion chromatography (SEC) and asymmetric flow field flow fractionation (AF4). Biological characterization included a series of bioassays (in vitro target binding, antibody-dependent cell-mediated cytotoxicity [ADCC], complement-dependent cytotoxicity [CDC] and apoptosis) and surface plasmon resonance (SPR) Fc receptor binding assays.

Results Intact mass analysis of GP2013 and the heavy and light chains using RP HPLC-ESI-MS revealed the expected molecular mass of rituximab. The amino acid sequence was shown to be identical between GP2013 and the originator rituximab. Further sequence confirmation using RP-HPLC-UV/MS peptide mapping showed non-distinguishable chromatograms for Lys-C digested GP2013 and originator rituximab. The higher order structure of GP2013 was shown to be indistinguishable from originator rituximab using a large panel of redundant and orthogonal methods. GP2013 and originator rituximab were comparable with regard to charge variants, specific amino acid modifications and the glycan pattern. GP2013 was also shown to have similar purity, aggregate and particle levels when compared with the originator. Functionally, and by using a comprehensive set of bioassays and binding assays covering a broad range of rituximab's functional activities, GP2013 could not be distinguished from originator rituximab.

Conclusion GP2013 was shown to be physicochemically highly similar to originator rituximab at the level of primary and higher order structure, post-translational modifications and size variants. An extensive functional characterization package indicated that GP2013 has the same biological properties as originator rituximab.

J. Visser (✉)

Sandoz Biopharmaceuticals, Hexal AG, Kelttenring 1 + 3,
82041 Oberhaching, Germany
e-mail: jan_marinus.visser@sandoz.com

I. Feuerstein · T. Stangler · T. Schmiederer · M. Schiestl
Sandoz Biopharmaceuticals, Sandoz GmbH, Kundl, Austria

C. Fritsch
Novartis Pharma AG, Basel, Switzerland

1 Background

Biosimilars are products that have been approved as being comparable or highly similar to existing biopharmaceuticals for which patents have expired. In Europe, the European Medicines Agency (EMA) has developed a specific regulatory pathway and has approved a number of biosimilars, including versions of human growth hormone, granulocyte colony-stimulating factor and epoetin. The EMA has also issued guidelines that describe non-clinical and clinical requirements for the development of biosimilar monoclonal antibodies (mAbs) [1]. Other countries have adopted similar regulatory frameworks containing the same basic principles as the European guidelines. In the USA, the Food and Drug Administration (FDA) released draft guidance for the regulatory review of biosimilars in early 2012 [2].

Biosimilar development involves an iterative target-directed approach leading to a manufacturing process that delivers a highly similar product. Subsequently, similarity to the originator product is demonstrated by a comprehensive comparability program. The first step and a key element of this comparison is extensive physicochemical and biological characterization, now possible using an array of state-of-the-art analytical techniques. On the basis of this characterization, a tailored pre-clinical and clinical program is designed to demonstrate and confirm biosimilarity. The regulatory process for the approval of biosimilars was derived from the same scientific principles and experiences with comparability exercises that manufacturers of originator drugs have to perform when implementing manufacturing changes. In this regard, changes in the manufacturing of originators have been shown to result in comparable products despite shifts in certain quality attributes. The resulting products were similar but not identical to the originally approved product [3].

Biosimilar development begins with a comprehensive characterization of the originator product to gain as much product understanding as possible. Because originator product characteristics can change over time, quality attributes of different originator batches are assessed over an extended period in order to define the originator product range to be used as a development target (or goal posts). Developing a biosimilar product is subsequently possible through target-directed development and requires understanding of the relationships between manufacturing process and product and between structure and function [4].

It is intended that the development of biosimilars will lead to more affordable biological treatments and so increase patient access to otherwise expensive therapies [5]. This may be especially so for therapeutic mAbs, the increasing use of which represents a major cost burden for health-care providers. One such treatment, rituximab [MabThera[®] (EU)/

Rituxan[®] (USA)], is currently indicated for the treatment of patients with non-Hodgkin's lymphoma and chronic lymphocytic leukemia, as well as rheumatoid arthritis and other autoimmune conditions. Rituximab is a chimeric mouse/human mAb consisting of a glycosylated immunoglobulin with human IgG1 constant regions and murine light-chain and heavy-chain variable region sequences. Here we report the physicochemical and biological characterization of a proposed biosimilar and originator rituximab.

2 Methods

Originator rituximab (Rituxan[®] and MabThera[®] 100 mg/10 ml or 500 mg/50 ml) batches were purchased from pharmacies and stored according to the manufacturer's instructions. The proposed biosimilar product, GP2013, was produced in-house at Sandoz Biopharmaceuticals. GP2013 drug product (100 mg/10 ml or 500 mg/50 ml) was used for all analyses shown, with the exception of the glycan analysis where drug substance was used. The reference material used for the bioassays was manufactured in-house to GMP (Good Manufacturing Practice) standard.

An array of routine analytical and extended characterization methods was used to compare rituximab originator batches with GP2013. The comparability test program was designed to ensure the detection of any physicochemical and functional differences according to regulatory (draft) guidelines [1]. X-ray crystallography and hydrogen deuterium exchange mass spectrometry (HDX-MS) were performed at Proteros Biostructures AG (Martinsried, Germany) and ExSAR (Monmouth Junction, NJ, USA), respectively. DSC measurements were conducted at LEK Pharmaceuticals d.d. (Menges, Slovenia). Bioassays and surface plasmon resonance (SPR) binding analysis were performed at Novartis AG (Basel, Switzerland). All other analyses were performed at Sandoz GmbH (Kundl, Austria).

2.1 Chromatography Systems

All chromatographic analyses were performed on Agilent 1100 or 1200 high-performance liquid chromatography (HPLC) systems (Böblingen, Germany) equipped with UV and fluorescence detection if not otherwise stated.

2.2 High-Performance Liquid Chromatography Electro-spray Ionization Mass Spectrometry (HPLC-ESI-MS)

Intact mass: The molecular masses of the GP2013 and reference batches were determined using a Q-TOF mass spectrometer (Synapt[®], Waters, Saint Quentin en Yvelines, France) after the heavy chain C-terminal lysine had been

enzymatically removed. The samples were desalted by reversed-phase chromatography using an Acquity UPLC (Waters, Manchester, UK) prior to MS analysis, and the mass spectrometer was calibrated. Raw protein spectra were deconvoluted before evaluation using the maximum entropy algorithm in the MassLynx software.

2.3 Non-reduced and Reduced Peptide Mapping with reversed-phase (RP)-HPLC-UV, -MS and -MS/MS

Peptide mapping with UV was performed to identify the primary sequences of tested products. Protein samples were digested using endoproteinase Lys-C (Wako, Osaka, Japan). Before Lys-C digestion, samples were either reduced with dithiothreitol (DTT) or not reduced to run the peptide map under reducing or non-reducing conditions, respectively. After digestion, the peptides were separated on a C18 reversed-phase column (Kinetex™ 2.6 μm C18 50 × 2.1 mm column, Phenomenex, Torrance, CA, USA). Detection was carried out at 214 nm or using MS equipped with electrospray ionization (Orbitrap, Thermo Scientific, Waltham, MA, USA).

2.4 Ellman's Assay

Free proteinogenic thiol groups were quantified by using Ellman's reagent (5,5'-dithiobis-(2-nitrobenzoic acid) [DTNB]). Ellman's reagent forms a mixed disulfide with thiols, liberating the chromophore 5-mercapto-2-nitrobenzoic acid (absorption maximum 410 nm, $\epsilon \sim 13.600 \text{ cm}^{-1} \text{ M}^{-1}$). Only thiol groups that are accessible to this water-soluble reagent are modified. For calibration, the tripeptide glutathione containing one free thiol group was used. This principle of measurement was applied to denatured samples.

2.5 Circular Dichroism (CD) Spectroscopy

CD experiments were carried out on a JASCO J-815 spectrometer (Jasco, Easton, MD, USA) equipped with a Peltier-type cell holder. Spectra were recorded at a temperature of 293 K, a scanning speed of 5 nm/min and a band width of 1 nm. Near UV CD spectra were recorded from 250 to 340 nm, and far UV CD spectra were recorded for the range 195–260 nm. For each sample, three scans were performed, and baseline correction was applied. Noise reduction and normalization of the spectrum was performed.

2.6 Fourier Transform Infra-Red (FTIR) Spectroscopy

FTIR measurements were performed using a CONFO-CHECK system with an AquaSpec flow-through transmission cell (Bruker, Rheinstetten, Germany). Resolution and measurement time were set to 4 cm^{-1} and 50 s, respectively.

2.7 Hydrogen Deuterium Exchange Mass Spectrometry (HDX-MS)

For HDX-MS, the GP2013 and originator rituximab samples were subjected to deuteration, after which the samples were acidified at 30, 100, 300, 1,000 and 3,000 s to quench the reaction. These samples were then passed over an immobilized pepsin column for digestion. For further MS analysis, peptic fragments were desalted on a reversed phase trap column and separated on a C18 column.

2.8 1D ^1H Nuclear Magnetic Resonance Spectroscopy (NMR)

1D proton NMR spectra were acquired at 298 K on a Bruker Avance III 500 MHz NMR system (Rheinstetten, Germany). The protein buffer was changed to 0.15 mM NaCl, 20 mM Na_2HPO_4 , 20 mM NaH_2PO_4 and 150 mM NaCl, pH 6.7, by molecular filtration. The Watergate sequence was used to suppress residual water signal. The protein samples used for NMR had a protein concentration of 0.15 mM. Spectra were recorded with a spectral width of 20 ppm; 8k scans were accumulated and then processed with Topspin 2.1 software.

2.9 X-Ray Analysis

For crystallization, GP2013 and the originator rituximab were digested with papain to separate the Fab and Fc part of the antibody. Fabs were isolated using anion exchange chromatography and protein A chromatography, and subsequently concentrated to 31 mg/ml. Crystallization trials were performed with approximately 1,200 different conditions and optimized for temperature, protein concentration, drop ratio, pH and precipitant concentrations. After crystallization, crystals were flash-frozen and measured at a temperature of 100 K. The X-ray diffraction data were collected from crystals of both Fab samples at the Swiss Light Source (Villigen, Switzerland) using cryogenic conditions. Data were processed using the XDS and XSCALE programs.

2.10 Differential Scanning Calorimetry (DSC)

DSC measurements were performed using an Auto Cap-DSC calorimeter (MicroCal, Northampton, MA, USA). Scans were recorded at a rate of $60 \text{ }^\circ\text{C/h}$. Samples were diluted to 1 mg/ml with reference buffer and scanned from 30 to $95 \text{ }^\circ\text{C}$.

2.11 Cation-Exchange Chromatography (CEX)

CEX separates protein variants based on their different charge and is highly selective with regard to product-

related variants of rituximab, being able to separate rituximab main compound from acidic and basic variants. Samples were either treated or untreated with carboxypeptidase B (CPB; Roche, Mannheim, Germany). Before injection, samples were cleaned and the concentration adjusted. CEX separation was performed using a weak CEX resin (ProPac WCX-10, 4 × 250 mm, Dionex, Germering, Germany), and samples were eluted using a linear gradient. UV detection took place at 280 nm.

2.12 Size Exclusion Chromatography (SEC), Capillary Electrophoresis with Sodium Dodecyl Sulfate (CE-SDS) and Asymmetric Flow-Field Flow Fractionation (AF4)

SEC, CE-SDS and AF4 were used to separate lower and higher molecular mass variants. SEC was performed using a TSK-Gel G3000SWXL column (Tosoh Bioscience, Stuttgart, Germany). Samples of rituximab (7.5 µg) were injected and UV detection carried out at 210 nm. CE-SDS under non-reducing conditions was performed on a Beckman PA800 Enhanced (Beckman Coulter, Brea, CA, USA). Samples were denatured, and any free sulfhydryl group from the cysteine side chain was alkylated with iodoacetamide to prevent disulfide shuffling before analysis. Samples were pressure-injected, and the separation was performed with -15 kV. UV absorbance was recorded at 214 nm. AF4 of GP2013 and reference batches was performed using a liquid chromatography system equipped with a UV detector from Agilent (Boeblingen, Germany) and a light-scattering and refractive detector from Wyatt (Santa Barbara, CA, USA). Separation was performed in a short channel using a 10 kDa regenerated cellulose membrane and 490 µm W spacer.

2.13 Boronate Affinity Chromatography

Separation of unglycated and glycosylated variants of GP2013 samples and reference material was performed employing an Agilent HPLC system equipped with a fluorescence detector. Samples were injected onto a TSK Boronate-5PW column (Tosoh Bioscience, Stuttgart, Germany) at 42 °C. Fluorescence excitation was monitored at 280 nm and emission at 345 nm.

2.14 Glycan Analysis

N-glycans were released from the Fc part of the mAbs using N-glycosidase F (Roche, Mannheim, Germany). Subsequent separation and concentration were performed by ultracentrifugal filtration and centrifugal evaporation. Excess 2-aminobenzamide (2-AB, Sigma-Aldrich,

Steinheim, Germany) was used to label the glycans. Free 2-AB label from derivatized glycans was removed by gel filtration using Sephadex G10 (GE Healthcare, Little Chalfont, UK). Normal phase chromatography, using a TSK-Gel Amide80 150 × 2.0-mm, 3-µm column (Tosoh Bioscience, Stuttgart, Germany), was employed to separate the 2-AB labeled glycans. A fluorescence detector, set at an excitation wavelength of 250 nm and emission wavelength 428 nm, recorded the eluting 2-AB labeled glycans.

2.15 SPR Fc Receptor Binding

The affinity to recombinant human Fcγ and FcRn receptors was determined by using a Biacore T200 (GE Healthcare, Freiburg, Germany). Recombinant Fcγ receptors of the FcγRI, FcγRII and FcγRIII families were immobilized covalently on carboxymethyl dextran-coated CM5 sensor chips using standard amine coupling chemistry. Analysis was then performed according to the manufacturer's recommendations. For FcRn binding, recombinant human FcRn was biotinylated enzymatically using a C-terminal Avi-tag sequence. Biotinylation was performed using recombinant biotin protein ligase (Avidity, Aurora, CO, USA) according to the manufacturer's recommendations. The solutions were injected on a previously untreated flow cell of a Series S SA sensor chip.

2.16 Functional Bioassays

Bioassays were developed as relative potency assays in which the activity of test samples was determined by comparison to an in-house reference standard. Relative potency was calculated using a parallel line assay design according to European (EP) and US Pharmacopoeia (USP) recommendations. In order to achieve highly meaningful data sets, all bioassays were developed for high precision with coefficients of variation of less than 10 %.

Binding of rituximab to CD20 was determined using a cell-based competitive binding assay in which test samples were used to displace a fluorescently labeled rituximab from the CD20 expressed on the surface of the human Raji B cell line. Binding of the fluorescently labeled agent to the cell surface is evaluated by flow cytometry. Binding to CD20 is a key prerequisite for subsequent downstream effects, including Fc-dependent effector functions and direct induction of target cell apoptosis.

In order to assess Fc-effector functions, antibody-dependent cell-mediated cytotoxicity (ADCC) and complement-dependent cytotoxicity (CDC) bioassays were developed. To quantify ADCC activity, fluorophore-labeled Raji B cells were incubated with rituximab in the presence of a human NK cell line. Fluorophore release

from dying target cells was quantified and used for calculation of relative potency. To assess CDC activity, Raji B cells were incubated with rituximab in the presence of rabbit complement, and target cell depletion was monitored by determining viable cell densities at the end of the incubation with a luminescent substrate.

The apoptosis bioassay measured the rituximab-induced externalization of phosphatidylserine on Raji B cells using Annexin V-FITC, while dead cells with permeabilized cell membranes were stained with propidium iodide.

3 Results and Discussion

GP2013 is produced in a genetically modified Chinese hamster ovary (CHO) cell line, which is a main work horse in the biopharmaceutical industry. The gene sequences for the mAb heavy and light chains were reverse-engineered from the amino acid sequence of the originator. During an extensive clone selection process, a production clone was chosen based on genetic stability, productivity and its quality attribute profile. The subsequently developed upstream process, which required many iterative cycles in order to obtain a quality attribute profile as close as possible to the originator, is performed in fed-batch mode. The downstream process, consisting of industry standard chromatographic purification and viral inactivation methods to manufacture the drug substance, was further optimized for the removal of process-related impurities. The process-related impurities in the drug substance (e.g., host cell protein, DNA) were not part of the comparability exercise because they are specific to the individual process. However, their residual levels comply with existing guidelines, compendia and other regulatory requirements, reflecting the fact that a state-of-the-art manufacturing process was developed. The drug substance is formulated to the final drug product using the same drug product formulation as the originator.

As comparability at the physicochemical and functional level is a prerequisite for establishing biosimilarity, an extensive state-of-the-art analytical toolbox (Table 1) was employed to characterize the proposed biosimilar rituximab GP2013 and show its comparability to originator rituximab.

A comprehensive selection of GP2013 quality attributes was analyzed and compared to the ranges of the originator quality attributes. The originator range was obtained by measuring several batches of the originator sourced in the EU (MabThera[®]) and the US (Rituxan[®]). When comparing MabThera[®] and Rituxan[®] batches, it was found that they were analytically indistinguishable. We also found that certain quality attributes of the originator (e.g., CEX and glycan profile) revealed a shift at one time point, which can most likely be attributed to a shift in the manufacturing

process [3]. The shift was observed for both MabThera[®] and Rituxan[®], which, together with being analytically indistinguishable, provides strong evidence that Rituxan[®] and MabThera[®] are derived from the same drug substance manufacturing process. The shift in quality attributes also means that reference material was on the market with pre-shift and post-shift quality, and has been used interchangeably. Because the label of the originator was not changed, the pre- and post-shift batches were obviously rated as comparable by the company and/or the regulators, which allows for the use of the combined quality attribute range for comparison. This approach is generally accepted by regulators as long as interactions between quality attributes are taken into account.

3.1 Physicochemical Characterization

3.1.1 Primary Structure

The confirmation of the primary structure is the cornerstone in the verification of the identity of GP2013 as rituximab. Intact mass analysis of intact GP2013 and the heavy and light chains using RP-HPLC-ESI-MS revealed the expected molecular mass of rituximab. Also the RP-HPLC-UV/MS peptide maps for Lys-C digested GP2013 and originator rituximab resulted in non-distinguishable chromatograms (Fig. 1). Final confirmation for the sameness of the amino acid sequence was obtained by using reduced peptide mapping followed by RP-HPLC-ESI-MS/MS sequencing, which resulted in 100 % sequence coverage.

3.1.2 Higher Order Structure

As structural elements of a protein determine its function, it is important that the higher order or 3D structure of a proposed biosimilar is thoroughly investigated by using a number of redundant and orthogonal methods. The disulfide bridging pattern of a mAb is one of the elements determining the higher order structure. Non-reducing RP-HPLC-ESI-MS peptide maps showed the expected disulfide bridging pattern in the originator product as well as GP2013. The following disulfide bridges were identified: intrachain [Cys(L23)-Cys(L87), Cys(L133)-Cys(L193), Cys(H22)-Cys(H96), Cys(H22)-Cys(H96), Cys(H148)-Cys(H204), Cys(H265)-Cys(H325), Cys(H371)-Cys(H429)] and interchain [Cys(L213)-Cys(H224), Cys(H230)-Cys(H230), Cys(H233)-Cys(H233)]. In addition, the total number of free thiols in both GP2013 and originator product was comparable and in the range of 0.3 mol/mol.

CD spectroscopy, measuring differences in the absorption of left-handed versus right-handed polarised light, was used to obtain information on the folding state of the

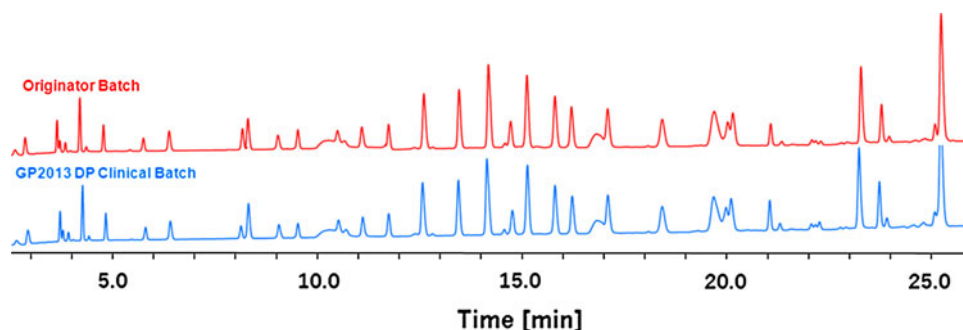
Table 1 An overview of the analytical toolbox used for the physicochemical and functional characterization of the proposed biosimilar GP2013 and originator rituximab

| Category | Quality attribute | Methods |
|--|--|---|
| Physicochemical characterization | | |
| Primary structure | Amino acid sequence | Red. RP-HPLC–ESI–MS peptide mapping, intact mass of whole mAB, HC and LC by RP-HPLC–ESI–MS, Red. RP-HPLC-UV peptide mapping |
| Higher order structure | Disulfide bridging | Non-red. RP-HPLC–ESI–MS peptide mapping |
| | Free thiols | Ellman's assay |
| | Secondary and tertiary structure | CD, FTIR, HDX-MS, X-ray |
| | Thermodynamic stability | DSC |
| General charge heterogeneity and amino acid modifications | OK variant, acidic variants, basic variant, Gln-variant, Lys-variant, amidated proline | CEX digested/undigested |
| | Glycation | Boronate affinity |
| | Oxidation/deamidation/C-terminal variants | RP-HPLC-UV/MS peptide mapping |
| Glycosylation | Galactosylation, sialylation, mannosylation, afucosylation, bisecting GlcNAc, NGNA, α -galactose, qualitative glycosylation pattern | NP-HPLC-FL |
| | Size heterogeneity | Monomer, low-molecular weight (LMW) and high molecular weight (HMW) variants (aggregates) |
| Heavy chain (HC), light chain (LC), aglycosylated HC, clipped variants | | Red. CE-SDS |
| Monomer, LMW (e.g., half antibodies (HL) and HHL variant) and HMW variants | | Non-red. CE-SDS |
| Subvisible particles | | Light obscuration (PhEur, $\geq 10 \mu\text{m}$ and $>25 \mu\text{m}$) |
| Visible particles | | Visual inspection (PhEur) |
| Functional characterization | | |
| Target and receptor binding | FcRn binding | SPR |
| | Fc γ R binding (Fc γ RIa, Fc γ RIIa, Fc γ RIIb, Fc γ RIIIa(F158), Fc γ RIIIa(V158), Fc γ RIIIb) | SPR |
| Bioactivity | CD20 target binding | Cell-based binding assay |
| | CDC potency | Cell-based CDC assay |
| | ADCC potency | Cell-based ADCC assay |
| | Apoptosis | Cell-based apoptosis assay |

protein. CD spectroscopy in the far and near UV spectral regions provides insight into the secondary structure (α -helix, β -sheet, random coil) and tertiary structure, respectively. CD spectra from GP2013 and the originator were shown to overlap indistinguishably. FTIR is an orthogonal method to CD, which provides information on the vibrational states of molecules. The protein backbone amide

groups generate a number of characteristic IR bands that can be used to determine protein backbone conformation. Again, GP2013 and originator FTIR spectra overlapped with no indication of structural differences.

A disadvantage of spectroscopic methods (e.g., CD, FTIR) is that they provide information of the folding state of proteins that are a global average of the entire structure.

Fig. 1 Comparison of UV chromatograms of Lys-C digested GP2013 and originator rituximab

Protein-labeling methods such as HDX-MS can be used to localise small differences in higher order structure at the level of peptides as the exchange process between deuterium and hydrogen is highly dependent on the local structural environment [6, 7]. Using HDX-MS, the same deuterium exchange-rate dynamics were observed for GP2013 and the originator product. In addition, 1D ^1H NMR spectroscopy was employed to compare GP2013 and originator rituximab. The principle of NMR is based upon the spin of nuclei with odd mass numbers in an external magnetic field. In a protein molecule, the individual electron environment of every proton is a direct consequence of the 3D fold of the protein. Unfortunately, mAbs are too large for complete structural determination of unlabeled proteins by routine NMR techniques. However, NMR can be used to obtain structural fingerprints, thereby providing information on the sameness of the 3D structure of the originator and the proposed biosimilar. GP2013 and rituximab originator NMR spectra were shown to be superimposable, with zooms of the aliphatic and amide region shown in Fig. 2.

To obtain even further insight into the protein's structure, X-ray crystallography was employed and the structure elucidated at the atomic level for GP2013 and originator product Fab fragments. The structures were solved and refined to a final resolution of 2.02 and 1.85 Å for the GP2013 Fab and originator rituximab Fab, respectively. For both structures the crystals were shown to contain two monomers of the respective Fab in the asymmetric unit. The model comprises residues Gln1 to Lys222 of the heavy chain (HC) and Gln1 to Gln212 of the light chain (LC). A superposition of the structures solved for both Fabs showed no significant deviations in the secondary and tertiary structures of the proteins. A root mean square deviation of 0.12 Å for the C_α atoms between the compared structures are within the experimental variants, and the structures can be considered identical (Fig. 3).

The thermodynamic stability of GP2013 and originator rituximab was compared by using DSC, a thermodynamic tool measuring the heat energy uptake that occurs in a sample with a regulated increase in temperature. Changes in the heat capacity of a sample result from the disruption of forces that stabilize the native protein structure, with the thermal transition temperatures (T_m) being indicative of a conformational change [8]. The DSC thermograms were found to be superimposable, with three partially overlapping transitions with T_m values of 71, 75 and 83 °C for both GP2013 and originator product. The three transitions are believed to be linked to the unfolding of the CH2, Fab and CH3 domain, respectively [9]. In addition, head-to-head stability studies at intended storage conditions (2–8 °C) revealed a comparable stability profile for GP2013 and originator.

By using a large panel of redundant and orthogonal methods, the higher order or 3D structure of GP2013 was shown to be indistinguishable from originator rituximab.

3.1.3 Charge Heterogeneity and Amino Acid Modifications

Charge variants may substantially affect the in vitro and in vivo properties of antibodies [10]. A highly sensitive and high-resolution CEX method was employed to separate protein variants based on their surface charges. The method is sensitive for the detection of C-terminal lysine heterogeneities as well as other acid and basic variants. The main charge variant in both GP2013 and originator product is the "0K" variant, an isoform with missing C-terminal lysine residues at the heavy chain and with N-terminal pyroglutamic acid residues. Acid and basic variants can be formed by chemical and enzymatic modifications [11], with the acidic fraction typically containing a variety of protein species such as deamidated, sialylated and glycosylated forms, while the basic fraction contains, e.g., oxidized and

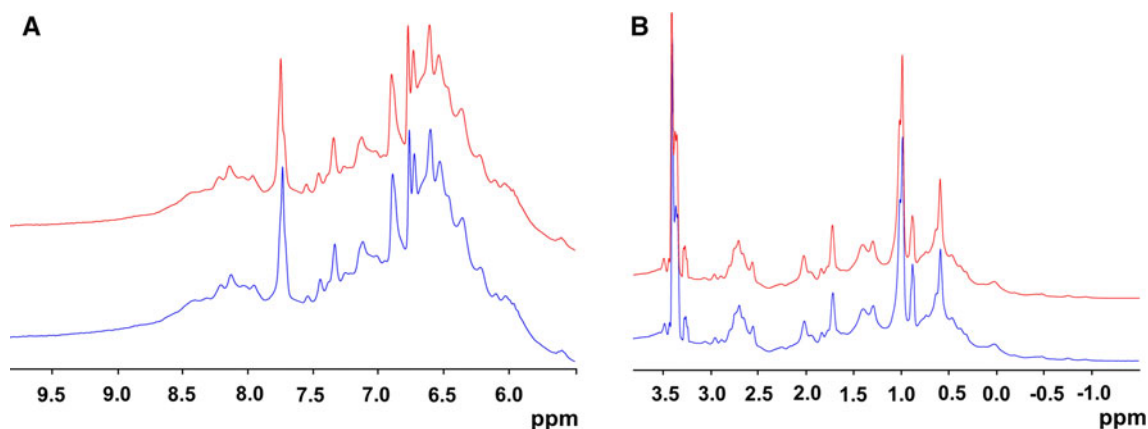


Fig. 2 Comparison of 1D ^1H NMR spectra of GP2013 and originator rituximab. *Blue line* GP2013; *red line* originator rituximab. **a** Zoom of the amide region of the NMR spectra. **b** Zoom of the aliphatic region of the NMR spectra

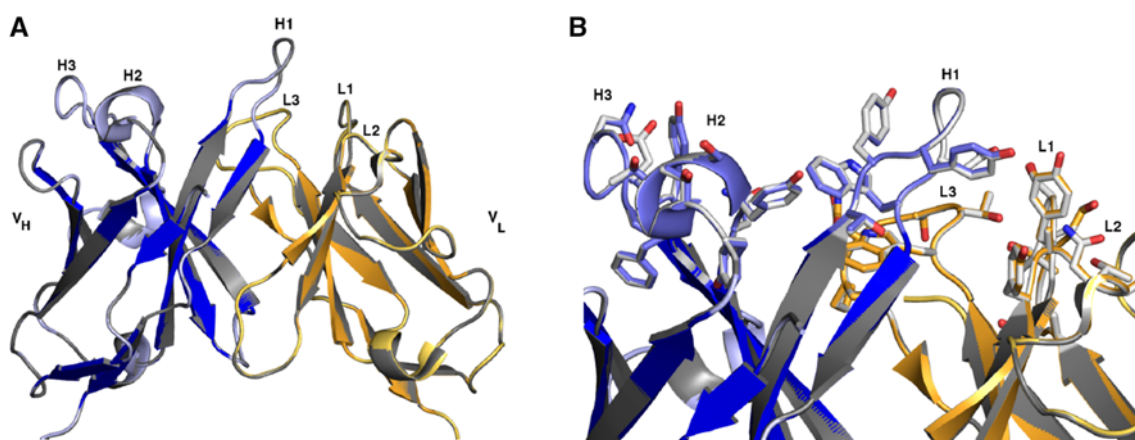


Fig. 3 Super-positioned view on the complementarity determining regions (CDRs) of GP2013 and originator rituximab. **a** Ribbon representation of the CDRs. The heavy chain and light chain structures of Fab GP2013 are colored in *blue* and *orange*, respectively. The structure of Fab originator rituximab is colored in *gray*.

b Ribbon representation of the CDRs with the side chains shown as a stick model, colored according to the chemical atom type (C GP2013 in *blue* and *orange*, C MabThera® in *gray*, O in *red*, and N in *blue*). CDR loops are labeled

C-terminal lysine variants. The sum of the GP2013 basic peaks was within the originator range, while the sum of the acid peaks was found to be slightly below the originator range (Fig. 4a).

Deamidation was further investigated by comparing deamidation of the Asn393 and Asn394 containing L28H peptide representing the prominent PENNYK deamidation hot spot [12] by using a RP-HPLC-UV peptide map. Deamidation was quantified by reporting the relative area percentage of the L28H isoaspartate peak relative to all L28H peptides and revealed approximately 0.5 % of deamidated L28H in GP2013 versus 1 % of deamidated L28H in originator rituximab (MabThera®). However, as a light increase in deamidation can be expected during DP shelf life, a lower level of deamidation may be desirable. The same peptide map was used to investigate oxidation of amino acid residue Met256 in more detail. Met256 is known to be easily oxidized [13] and is contained within the L17H peptide. The oxidized peptide L17Hox can be easily separated from the other peptides, and it was shown that both GP2013 and originator rituximab contained values <0.2 % relative to the total L17H peptide.

Treatment of mAbs with CPB removes C-terminal lysine heterogeneity and allows for more easily interpretable CEX chromatograms. However, CEX chromatograms of CPB-digested GP2013 and originator product suggested the presence of a basic C-terminal modification at $t = 22$ min in GP2013, which is not present in the originator product (Fig. 4b). Indeed, and by using peptide mapping MS, this particular modification was identified as amidated proline (AP; P-NH₂) and quantified to be present at a level <2 % in GP2013, while being below the limit of detection in originator rituximab. AP is formed when the

C-terminal lysine and glycine residues are removed and the exposed proline residue amidated. AP was first detected on a mAb by Johnson et al. [14], who showed no effect on Fab binding and Fc effector function. The latter is also to be expected as AP is located at the C-terminus of the mAb and therefore far removed from any binding or effector function relevant part. However, and in order not to solely rely on the literature data, GP2013-specific data were generated showing that (1) GP2013 AP-enriched material had the same functional properties as originator rituximab when tested in bioassays (binding, ADCC and CDC), (2) the use of 9 % AP-containing GP2013 material in an animal pharmacokinetic study resulted in AUC and C_{\max} values comparable to the originator and (3) a repeated-dose toxicity study in cynomolgus monkeys comparing 9 % AP-containing GP2013 material with originator rituximab revealed no detectable differences in safety profile between the test and reference items. This step-wise approach is in line with the approach advocated by regulators and justifies the small qualitative difference.

Another amino acid modification is glycation. Glycation is the chemical modification of lysine residues by glucose, which is a reducing sugar and reacts with free amines, after which the reaction product undergoes rearrangement to form a stable ketoamine [15]. Boronate affinity chromatography, which retains fractions containing *cis*-hydroxyl groups found in the stable ketoamine, was used to determine the relative amount of glycated mAbs. Both GP2013 and reference product were found to contain approximately 2–3 % glycated species.

When looking at charge variants in general and specific amino acid modifications in particular, it can be concluded that GP2013 and originator rituximab are comparable.

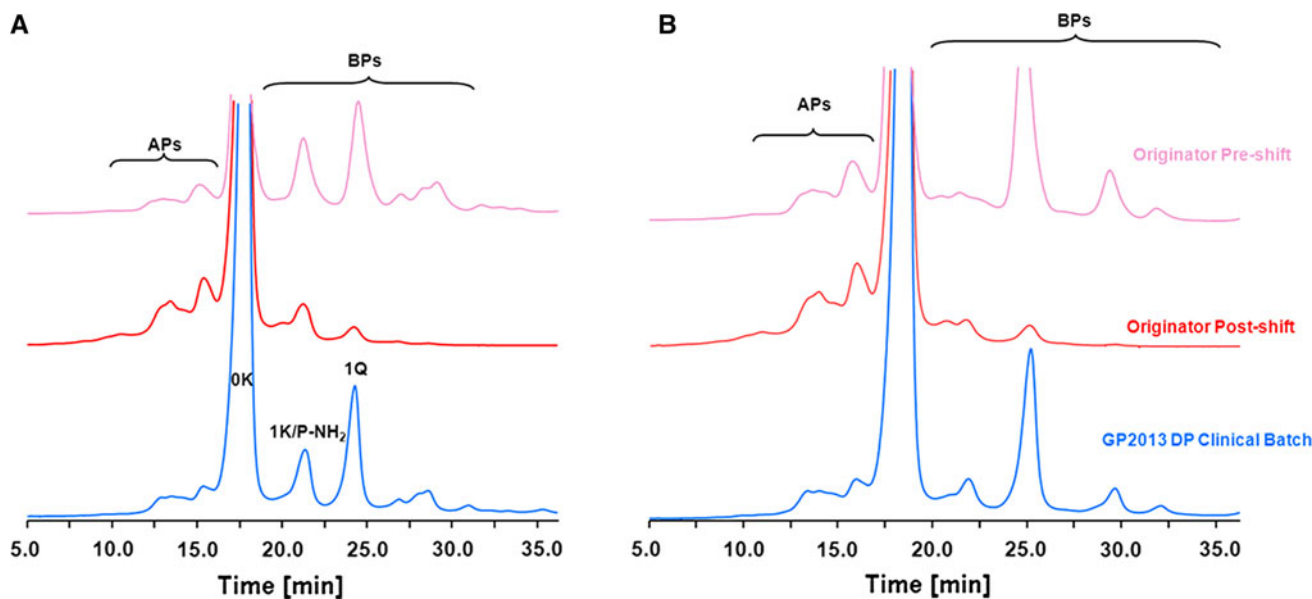


Fig. 4 Cation exchange chromatograms of GP2013 and originator rituximab (a) and after carboxypeptidase B (CPB) digest (b). As at

one point in time changes in originator CEX-profiles were observed, both pre-shift and post-shift material is depicted

3.1.4 Glycosylation

Glycans can play an important role in determining the efficacy and *in vivo* half-life of mAbs [16]. Peptide mapping confirmed the glycosylation site of GP2013 and the reference product to be at Asn(301), while reduced CE-SDS revealed that in both molecules >99 % of Asn301 was glycosylated. Glycans were enzymatically released from the mAbs by the enzyme PNGaseF and identified by 2-AB labeling followed by normal-phase HPLC with fluorescence detection. Using MS, 25 glycan species were identified on GP2013, all of which are also present on the reference product. No potentially immunogenic glycoforms [17] such as NGNA [18] or Gal- α -1,3 Gal [19, 20] could be identified. The glycosylation pattern of the major abundant glycans, such as the bG0, bG1 (1,6_bG1 and 1,3_bG1) and bG2 isoforms, was very comparable between GP2013 and the reference product (Fig. 5a). When looking at the low-abundant glycan structures, small differences could be identified (Fig. 5b).

The heterogeneity of low-abundant glycans was lower in GP2013 when compared to originator, with the minor glycans bNG1 and bG1S1 only being identified in originator rituximab. GP2013 was also shown to contain slightly lower amounts of mannose structures (Man 5, M7, M8, M9) of around 1 %, while the originator values ranged between 1.7–5.4 %. Unfucosylated glycan structures are known to influence ADCC activity [21–23], with the unfucosylated bG0 structure playing a major role. As ADCC represents one of the main modes of action of rituximab,

significant attention was paid to the unfucosylated bG0 structure during cell line and process development. The originator range was shown to vary between 0.3–1.8 %. However, GP2013 was designed to contain approximately 1.4 % of unfucosylated bG0, which resulted in an ADCC activity in the middle of the originator range (see Sect. 3.2).

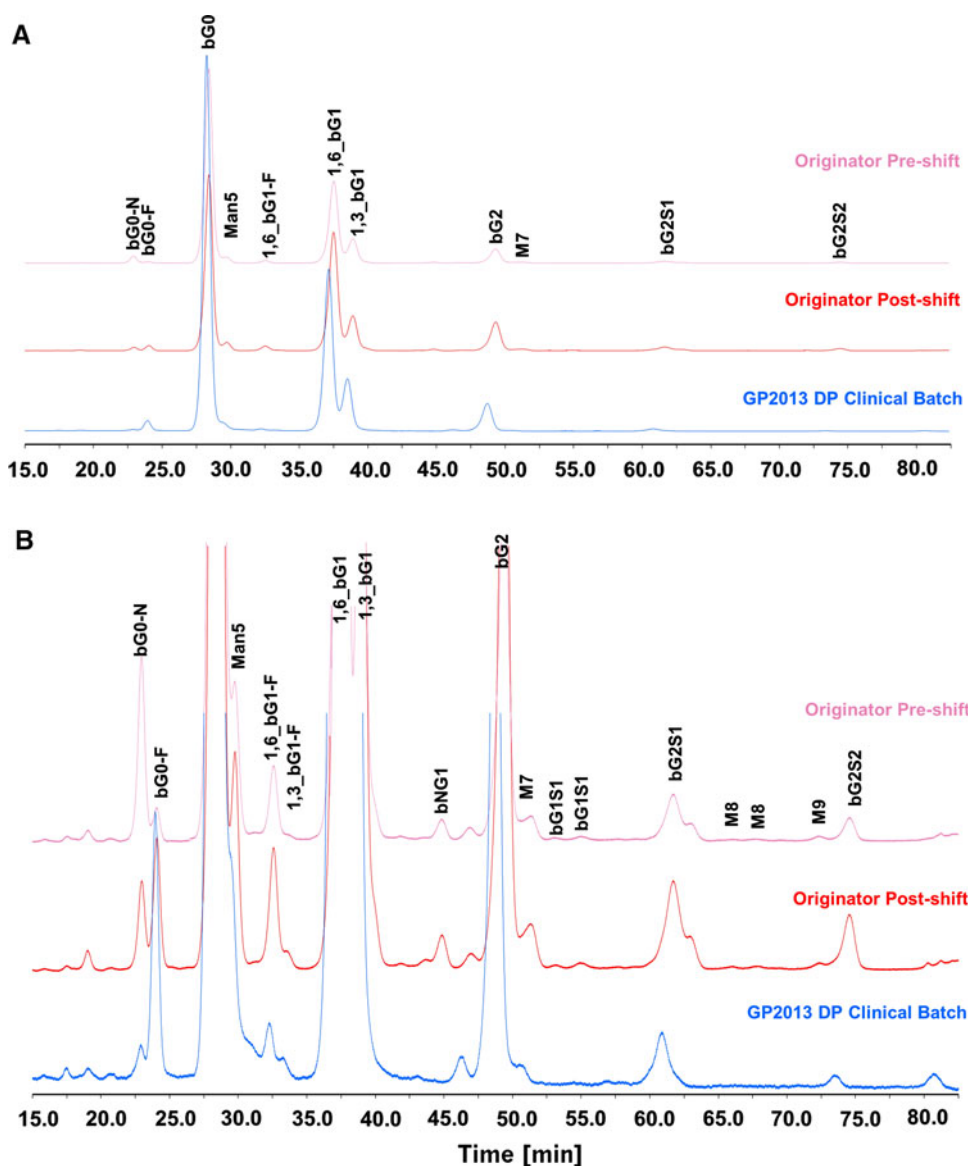
Overall, and despite some minor differences in some low-abundant glycan species, it can be concluded that the glycan pattern of GP2013 is comparable to the reference product.

3.1.5 Size Heterogeneity

Size matters in biological medicinal products, especially as aggregates have been implicated in enhancing immunogenicity and affecting safety and efficacy [24, 25]. Reducing CE-SDS resolved the light chain, heavy chain and non-glycosylated heavy chain from impurities by size. Similar chromatographic profiles and purity values of >98 % were found for GP2013 and originator product. Non-reducing CE-SDS was used to separate monomers from fragments and higher molecular weight variants. In the electropherograms of GP2013 and originator products, a number of minor variants were resolved and detected. The amounts of free light chain (L), free heavy chain (H) and of half antibody (HL) were below the quantitation limit. A variant with one missing light chain (HHL) was detected at values of around 1.5 % for both GP2013 and originator (Fig. 6).

SEC under native conditions separates monomeric mAbs from other variants of lower or higher molecular

Fig. 5 Glycosylation pattern of GP2013 and originator rituximab—extended view (a) and zoomed view (b). As at one point in time changes in originator glycan profiles were observed, both pre-shift and post-shift material is depicted



weight by differential exclusion from the pores of the packing material. The retention times of monomeric GP2013 and originator product were the same, while purity results were >98 % for the originator product and >99 % for GP2013. There was also no indication of different types of higher molecular weight variants. Based on the potential importance of aggregates, AF4 was used as an orthogonal method to SEC. Within AF4, high-resolution separation of size variants is achieved using a very thin flow against which a perpendicular force field is applied. The AF4 results were found to be comparable with the SEC results, confirming that GP2013 and originator rituximab have the same purity and level of aggregates.

Compendial limits for the number of sub-visible particles per container are defined at 6,000 for particles $\geq 10 \mu\text{m}$ and 600 for particles $\geq 25 \mu\text{m}$ as measured by light obscuration (EP 2.9.19 and USP <788>). GP2013 was

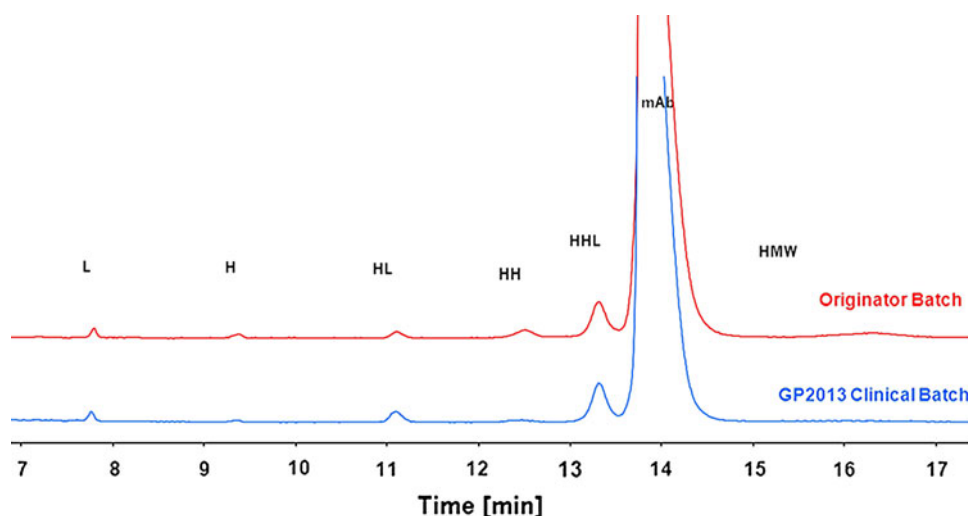
found to meet the regulatory criteria with values of <200/container and <5/container for particles of ≥ 10 and $\geq 25 \mu\text{m}$, respectively. In line with originator rituximab, GP2013 was also found to be practically free of visible particles as assessed by visual inspection according to the EP 2.9.20 monograph.

Overall it can be concluded that GP2013 has a similar purity, aggregate and particle level when compared to the originator.

3.2 Functional Characterization

Rituximab binds the CD20 antigen on the surface of B cells and has three main elements that contribute to its mode of action of killing the targeted B-cell once binding to CD20 has been achieved [26]. These main contributors are (1) CDC, (2) ADCC and (3) direct induction of apoptosis

Fig. 6 Electropherograms of non-reduced GP2013 and originator rituximab. Zoomed view of the electropherograms on the rituximab-related subunit corresponding to light chain (L), heavy chain (H), heavy-light chain (HL), heavy-heavy chain (HH), heavy-heavy-light chain (HHL) and high molecular weight variants (HMW)



through binding of CD20. Since it is not fully established how these main mechanisms of action of rituximab contribute to safety and efficacy *in vivo*, a comprehensive set of potency bioassays was developed to provide a complete picture of GP2013's functional integrity and comparability to the originator.

3.2.1 Bioassays

A prerequisite for all further downstream actions that combine to cause B cell depletion *in vivo*, the binding of GP2013 to its target CD20 was assessed in a cell-based competitive binding assay and was found to be well within the originator range (Table 2). This was expected given that GP2013 has not only the same primary and higher order structure as the originator product, but also a highly similar profile with respect to post-translational modifications.

The activity of GP2013 was further compared to originator rituximab in CDC and ADCC assays, which depend on a fully functional Fc domain in addition to target binding. GP2013 was seen to be comparable to originator rituximab in CDC and ADCC assays (Table 2). It is known that variable Fc glycosylation can influence the activity of mAbs in both CDC and ADCC assays, with the latter assay typically showing a high sensitivity to the presence of defucosylated glycans. Interestingly, the variability of originator rituximab in the ADCC assay was significantly higher than its variability in the CDC assay.

Finally, the direct induction of apoptosis caused by the binding of rituximab to CD20 was quantified in a bioassay based on the rituximab-induced externalization of phosphatidylserine on Raji B cells. Also in this assay, the activity of GP2013 was comparable to the originator (Table 2).

The results from all potency bioassays were assessed for bioequivalence using the two-sided test procedure (TOST) and applying the usual bioequivalence limits of 0.8–1.25.

The corresponding *p* values were all highly significant (<0.0001) confirming bioequivalence between GP2013 and the reference product.

3.2.2 SPR binding assays

SPR was used to determine the affinity of GP2013 and reference product to recombinant human Fc γ and FcRn receptors. The neonatal Fc receptor for IgG is expressed by endothelial cells and monocytes, which recycle IgG into circulation, and therefore impacts serum half-life [27]. Fc γ Rs are mostly expressed on leukocytes and are relevant for the function of therapeutic antibodies [28]. Three types of Fc γ R are present in humans (Fc γ RI, Fc γ RII and Fc γ RIII), and they differ in the type of signaling pathway they trigger and their affinity to IgGs [29]. Especially Fc γ RIIIa is implicated in inducing ADCC, and patients with follicular lymphoma who carried the higher affinity variant Fc γ RIIIa V158 have been shown to have higher response rates to rituximab [30]. The affinity constants obtained for the different types of Fc γ Rs (Table 3) are in line with what is

Table 2 GP2013 potency values as measured in the *in vitro* target binding, ADCC, CDC and apoptosis bioassay in comparison to the originator range. Bioassays are performed in duplicate. The originator range reflects the minimum and maximum value of 59 batches for the ADCC, 62 batches for the CDC bioassay, 48 batches for target binding and 7 batches for the apoptosis bioassay, which was developed later. The range stated for GP2013 reflects the minimum and maximum value of 11 clinic batches for binding, ADCC and CDC and 5 batches for the apoptosis assay

| | Target binding | ADCC | CDC | Apoptosis |
|-----------------------|----------------|---------|---------|-----------|
| GP2013 (%) | 97–108 | 86–105 | 99–111 | 88–97 |
| Reference range (%) | 96–110 | 70–132 | 95–127 | 88–102 |
| <i>p</i> value (TOST) | <0.0001 | <0.0001 | <0.0001 | <0.0001 |

Table 3 GP2013 affinity constants (K_D) for binding to the FcRn and Fc γ R receptors in comparison to the originator range as determined by surface plasmon resonance. Per sample the affinity to each receptor was determined four times. The data shown were performed head to head and reflect the minimum and maximum value of seven originator batches and five GP2013 clinical batches

| | Reference K_D | GP2013 K_D |
|------------------------|-------------------|-------------------|
| FcRn | 0.55–0.58 μ M | 0.54–0.58 μ M |
| Fc γ RIa | 10.4–11.8 nM | 10.9–12.4 nM |
| Fc γ RIIa | 2.4–2.7 μ M | 2.4–2.7 μ M |
| Fc γ RIIb | 11.4–12.8 μ M | 11.0–12.7 μ M |
| Fc γ RIIIa F158 | 7.4–10.3 μ M | 8.5–10.9 μ M |
| Fc γ RIIIa V158 | 3.5–4.9 μ M | 4.2–5.0 μ M |
| Fc γ RIIIb | 9.2–11.7 μ M | 9.9–12.4 μ M |

typically found in the literature [31–33]. Even more importantly, it was shown that the affinity of GP2013 towards FcRn and Fc γ Rs was very comparable to the affinity the originator product displayed.

By using a comprehensive set of bioassays and binding assays, covering rituximab's possible mode of actions, GP2013 could not be functionally distinguished from the reference product.

4 Conclusions

MAbs are large and complex proteins, but it is possible to characterize them in great detail by using an extensive set of state-of-the-art analytical technologies. The use of orthogonal methods minimizes the risk of missing relevant modifications, while the combination of all analytical techniques provide a very comprehensive picture of the molecule. Physicochemically, GP2013 was shown to be highly similar to originator rituximab at the level of primary and higher order structure, post-translational modifications and size variants. An extensive functional characterization package, including SPR-based binding assays and in vitro cell-based bioassays, revealed that GP2013 has the same biological properties as the originator rituximab. Despite not knowing the originator process and using a different CHO cell line and different upstream and downstream manufacturing process, it was possible to create a mAb (GP2013) highly similar to originator rituximab at the level of individual quality attributes and indistinguishable from a functional perspective. This demonstrates that target-directed biosimilar development of complex molecules such as mAbs is possible.

A thorough physicochemical and functional comparability exercise serves as a foundation for the subsequent demonstration of biosimilarity in further pre-clinical and clinical trials. A high level of structural and functional

similarity provides confidence that tailored pre-clinical and clinical studies will also reveal a comparable safety and efficacy profile. Indeed, a subsequent pre-clinical comparability exercise confirmed that GP2013 and originator rituximab are pharmacologically comparable with regard to anti-tumor activity, PK exposure (AUC and C_{max}) and B-cell depletion. As such, it can also be anticipated that GP2013 will show comparable potency and safety as the reference product in ongoing clinical trials (ClinicalTrials.gov NCT01274182 and NCT01419665), bringing the availability of more affordable biologics a step closer.

Acknowledgments Sandoz, a Novartis company, funded all analyses. The analytical program set-up, management and/or execution of the analyses and the subsequent interpretation of analytical data were done by the authors and members of the GP2013 project team. The entire GP2013 project team is acknowledged for their contribution to the development of GP2013. The authors also would like to acknowledge Dr. Jacki Kornbluth, St. Louis University, for providing the NK cell line NK3.3. Medical writing support was provided by Andy Bond of Spirit Medical Communications Ltd., supported by Sandoz.

Open Access This article is distributed under the terms of the Creative Commons Attribution Noncommercial License which permits any noncommercial use, distribution, and reproduction in any medium, provided the original author(s) and the source are credited. The exclusive right to any commercial use of the article is with Springer.

References

1. European Medicines Agency, Committee for Medicinal Products for Human Use (CHMP). Guideline on similar biological medicinal products containing monoclonal antibodies—non-clinical and clinical issues. London: European Medicines Agency; 2012. http://www.ema.europa.eu/docs/en_GB/document_library/Scientific_guideline/2012/06/WC500128686.pdf.
2. Food and Drug Administration, Center for Drug Evaluation and Research (CDER). Guidance for Industry. Scientific considerations in demonstrating biosimilarity to a reference product. Rockville: Food and Drug Administration; 2012. <http://www.fda.gov/downloads/Drugs/GuidanceComplianceRegulatoryInformation/Guidances/UCM291128.pdf>.
3. Schiestl M, Stangler T, Torella C, et al. Acceptable changes in quality attributes of glycosylated biopharmaceuticals. *Nat Biotechnol.* 2011;29(4):310–2.
4. McCamish M, Woollett G. The state of the art in the development of biosimilars. *Clin Pharmacol Ther.* 2012;91(3):405–17.
5. Cornes P. The economic pressures for biosimilar drug use in cancer medicine. *Target Oncol.* 2012;7(Suppl 1):S57–67.
6. Engen JR. Analysis of protein confirmation and dynamics by hydrogen/deuterium exchange MS. *Anal Chem.* 2009;81(19):7870–5.
7. Houde D, Berkowitz SA, Engen JR. The utility of hydrogen deuterium exchange mass spectrometry in biopharmaceutical comparability studies. *J Pharm Sci.* 2011;100(6):2071–86.
8. Van Holde KE, Curtis Johnson W, Shing Ho P. Thermodynamics and biochemistry. In: Principles of physical biochemistry. 2nd ed. Upper Saddle River: Pearson Prentice Hall; 2006. p. 72–105.
9. Andersen CB, Manno M, Rischel C, Thóroffsson M, Martorana V. Aggregation of a multidomain protein: a coagulation

- mechanism governs aggregation of a model IgG1 antibody under weak thermal stress. *Prot Sci*. 2010;19:279–90.
10. Du Y, Walsh A, Ehrick R, et al. Chromatographic analysis of the acidic and basic species of recombinant monoclonal antibodies. *MAbs*. 2012;4(5):578–85.
 11. Khawli LA, Goswami S, Hutchinson R, et al. Charge variants in IgG1: isolation, characterization, in vitro binding properties and pharmacokinetics in rats. *MAbs*. 2010;2(6):613–24.
 12. Chelius D, Rehder DS, Bondarenko PV. Identification and characterization of deamidation sites in the conserved regions of human immunoglobulin gamma antibodies. *Anal Chem*. 2005;77(18):6004–11.
 13. Chumsae C, Gaza-Bulsecu G, Sun J, et al. Comparison of methionine oxidation in thermal stability and chemically stressed samples of a fully human monoclonal antibody. *J Chromatogr B Analyt Technol Biomed Life Sci*. 2007;850(1–2):285–94.
 14. Johnson KA, Paisley-Flango K, Tangarone BS, et al. Cation exchange-HPLC and mass spectrometry reveal C-terminal amidation of an IgG1 heavy chain. *Anal Biochem*. 2007;360(1):75–83.
 15. Zhang B, Yang Y, Yuk I, et al. Unveiling a glycation hot spot in a recombinant humanized monoclonal antibody. *Anal Chem*. 2008;80(7):2379–90.
 16. Hossler P, Khattak SF, Li ZJ. Optimal and consistent protein glycosylation in mammalian cell culture. *Glycobiology*. 2009;19(9):936–49.
 17. Beck A, Wagner-Rousset E, Bussat MC, et al. Trends in glycosylation, glycoanalysis and glycoengineering of therapeutic antibodies and Fc-fusion proteins. *Curr Pharm Biotechnol*. 2008;9(6):482–501.
 18. Ghaderi D, Taylor RE, Padler-Karavani V, et al. Implications of the presence of *N*-glycolylneuraminic acid in recombinant therapeutic glycoproteins. *Nat Biotechnol*. 2010;28(8):863–7.
 19. Macher BA, Galili U. The Galalpha1,3Galbeta1,4GlcNAc-R (alpha-Gal) epitope: a carbohydrate of unique evolution and clinical relevance. *Biochim Biophys Acta*. 2008;1780(2):75–88.
 20. Chung CH, Mirakhor B, Chan E, et al. Cetuximab-induced anaphylaxis and IgE specific for galactose- α -1,3-galactose. *N Engl J Med*. 2008;358(11):1109–17.
 21. Shields RL, Lai J, Keck R, et al. Lack of fucose on human IgG1N-linked oligosaccharides improves binding to human Fcgamma RIII and antibody-dependent cytotoxicity. *J Biol Chem*. 2002;277(30):26733–40.
 22. Niwa R, Natsume A, Uehara A, et al. IgG subclass-independent improvement of antibody-dependent cellular cytotoxicity by fucose removal from Asn297-linked oligosaccharides. *J Immunol Methods*. 2005;306(1–2):151–60.
 23. Chung S, Quarmby V, Gao X, et al. Quantitative evaluation of fucose reducing effects in a humanized antibody on Fc receptor binding and antibody-dependent cell-mediated cytotoxicity activities. *MAbs*. 2012;4(3):326–40.
 24. Rosenberg AS. Effects of protein aggregates: an immunologic perspective. *AAPS J*. 2006;8(3):E501–7.
 25. den Engelsman J, Garidel P, Smulders R, et al. Strategies for the assessment of protein aggregates in pharmaceutical biotech product development. *Pharm Res*. 2011;28(4):920–33.
 26. Weiner GJ. Rituximab: mechanism of action. *Semin Hematol*. 2010;47(2):115–23.
 27. Roopenian DC, Akilesh S. FcRn: the neonatal Fc receptor comes of age. *Nat Rev Immunol*. 2007;7(9):715–25.
 28. Jiang XR, Song A, Bergelson S, et al. Advances in the assessment and control of the effector functions of therapeutic antibodies. *Nat Rev Drug Discov*. 2011;10(2):101–11.
 29. Nimmerjahn F, Ravetch JV. Anti-inflammatory actions of intravenous immunoglobulin. *Annu Rev Immunol*. 2008;26:513–33.
 30. Cartron G, Dacheux L, Salles G, et al. Therapeutic activity of humanized anti-CD20 monoclonal antibody and polymorphism in IgG Fc receptor FcgammaRIIIa gene. *Blood*. 2002;99(3):754–8.
 31. Mimura Y, Sondermann P, Ghirlando R, et al. Role of oligosaccharide residues of IgG1-Fc in Fc γ RIIb binding. *J Biol Chem*. 2001;276(49):45539–47.
 32. Masuda K, Kubota T, Kaneko E, et al. Enhanced binding affinity for Fc γ RIIIa of fucose-negative antibody is sufficient to induce maximal antibody-dependent cellular cytotoxicity. *Mol Immunol*. 2007;44(12):3122–31.
 33. Lee CH, Choi DK, Choi HJ, et al. Expression of soluble and functional human neonatal Fc receptor in *Pichia pastoris*. *Prot Expr Purif*. 2010;71(1):42–8.